CrossMark

INVITED REVIEW

This section of Journal of Materials Research is reserved for papers that are reviews of literature in a given area.

Cold sintering: Current status and prospects

Jon-Paul Maria, Xiaoyu Kang, Richard D. Floyd, and Elizabeth C. Dickey
Department of Materials Science and Engineering, North Carolina State University, Raleigh 27695, North Carolina, USA

Hanzheng Guo, Jing Guo, and Amanda Baker
Department of Material Science and Engineering, Materials Research Institute, The Pennsylvania State University, University Park 16802, Pennsylvania, USA

Shuichi Funihashi
Department of Material Science and Engineering, Materials Research Institute, The Pennsylvania State University, University Park 16802, Pennsylvania, USA; and Murata Mfg. Co., Ltd., Nagaokakyo-shi, Kyoto, Japan

Clive A. Randall[a)]
Department of Material Science and Engineering, Materials Research Institute, The Pennsylvania State University, University Park 16802, Pennsylvania, USA

(Received 16 January 2017; accepted 14 June 2017)

This manuscript describes, defines, and discusses the process of cold sintering, which can consolidate a broad set of inorganic powders between room temperature and 300 °C using a standard uniaxial press and die. This temperature range is well below that needed for appreciable bulk diffusion, indicating immediately the distinction from the well-known and thermally driven analogue, allowing for an unconventional method for densifying these inorganic powders. Sections of this report highlight the general background and history of cold sintering, the current set of known compositions that exhibit compatibility with this process, the basic experimental techniques, the current understanding of physical mechanisms necessary for densification, and finally opportunities and challenges to expand the method more generically to other systems. The newness of this approach and the potential for revolutionary impact on traditional methods of powder-based processing warrants this discussion despite a nascent understanding of the operative mechanisms.

I. INTRODUCTION

Sintering is the process by which a particle compact, referred to commonly as a green body, is transformed to a physically robust and dense polycrystalline monolithic by the application of heat.[1–3] The transformation is driven by the energetic return that accompanies curvature reduction, creating grain boundaries, and eliminating solid–vapor interfaces. For a 1 μm particle compact, the driving force for sintering is on the order of 10^2 J/mol, or about 10^3 times smaller than the formation energies of typical inorganic solid crystals.[1–3] Since the sintering transformation requires bulk diffusion of atoms from the particle interiors to the inter-particle necks, in most cases temperatures between 1/2 and 3/4 of the melting point are needed. These high temperatures are restrictive in the context of material integration, material synthesis, phase stability, and net shape formation, and contribute substantially to the energy budget for processing.

For many years, the materials synthesis and processing communities have sought opportunities to minimize sintering temperatures, ideally to a range below 300 °C, at which point integration with polymeric and non-noble metals becomes feasible. In addition, at this low temperature range, conventional stainless steel fixtures and formation dies are stable in contact with many inorganic oxides, nitrides, and carbides in a variety of atmospheres. Many techniques are explored to accomplish this goal, including liquid phase additions, sintering at high pressures, and applying large electric fields. There is particular interest for sintering in the presence of electric fields; namely, techniques such as Field Assisted Sintering Technology (FAST), Spark Plasma Sintering (SPS), and FLASH sintering.[4–10] In these cases, sintering is induced by heating the ceramic powders at interfaces through processes such as local Joule heating, however there is a substantial debate regarding the predominant mechanisms. While each method above appreciates some success, none have

Contributing Editor: Eugene Medvedovski
[a)]Address all correspondence to this author.
e-mail: car4@psu.edu
DOI: 10.1557/jmr.2017.262

 © Materials Research Society 2017

https://doi.org/10.1557/jmr.2017.262 Published online by Cambridge University Press

pushed the temperature window into the desired low-temperature range.

In 1986, Yamasaki published the first report describing the combination of hydrothermal processing and isostatic pressing to densify ceramic bodies at temperatures below 200 °C.[11] Following these early reports, this hydrothermal hot pressing (HHP) concept generated modest interest in the context of hydroxyapatite/metal bonding and attempts to densify compositions that decompose at temperatures well below that needed for sintering. More recently, a series of several reports expanded this original work to a broad series of electronic and technical ceramics, with high purity, that in multiple cases can exceed 90% theoretical density in the same temperature range. Composite structures, both ceramic–ceramic and polymer–ceramic, were also demonstrated.[12–28] All of these approaches share a processing similarity where a small volume fraction of liquid phase is added to the starting powders, providing a medium for mass transport by a combination of dissolution, precipitation, and nucleation that are assisted/enabled by applied pressure and heat. This expanded process is referred to as the "cold sintering process" (CSP) since the active temperature window spans the range from room temperature to 300 °C.

In this manuscript, the authors provide a summary of the CSP and its relation to other consolidation methods; a discussion of current hypotheses that explain the operative phenomena; and an initial perspective regarding the potential impact on ceramic processing, energy consumption, and applications. While the current understanding of cold sintering is nascent and likely to change as experiments progress, the potentially transformative outcomes of the process warrant this early perspective.

II. CSP BACKGROUND

We define CSP as the process where an inorganic powder is densified in the presence of a transient liquid phase at a phase fraction typically between 1 and 10 vol%.[12–28] During cold sintering, the liquid phase becomes the medium for mass transport. Consequently, this liquid should be pre-loaded with the cation and anion species that comprise the solid in solution, or the solid particles should exhibit finite congruent solubility in it. While water is the most common cold sintering liquid, many other organic and ionic liquids can be used. The moist powder is subsequently loaded into a conventional pellet die to which mechanical force and heat are applied. Pressures and temperatures typically span the range between 100 and 500 MPa and 25–300 °C, respectively. In some cases the applied pressure can be eliminated. However, the optimal rates and times for pressure and temperature application are material-specific.

It is important to note that other researchers explored similar possibilities for low temperature densification, most notably the research group of Kanahara at the Research Laboratory of Hydrothermal Chemistry at Kochi University, who first combined hydrothermal reactions with uniaxial pressure in 1986. Inspired by the natural geological phenomenon of lithification, Yamasaki et al. reported the process of HHP.[11] While very few details of final microstructure, material properties, or densification mechanisms were provided, they included an important and detailed description of the instrumentation, they observed the requirement of liquid escape, and they discussed processing pressure and temperature ranges of interest. Yamasaki and co-workers published a number of additional reports on materials including TiO_2, $CaCO_3$, and SiO_2, but focused primarily on consolidating compositions that decomposed at high temperatures, or preparing porous bodies with fine control of pore sizes.[29–32] In perhaps the first demonstration of full density, Sato et al. applied HHP to $Sn_{1.24}Ti_{1.94}O_{3.66}(OH)_{1.5}F_{1.42}$, which cannot be densified conventionally as it decomposes at 300 °C. They were able to produce nearly phase-pure samples and provided one of the earliest reports of 99% theoretical density.[33] Very recently, Bouville and Studart reported cold sintering of nano-$CaCO_3$ powders at room temperature, indicating promising mechanical properties, especially under compressive stress.[34]

There also exists an important relative body of work involving reactive hydrothermal synthesis. $BaTiO_3$ provides a well-known example where fine ceramic powders are formed from a Ti- or TiO_2-based precursor that reacts with a Ba-source under hydrothermal conditions. Numerous authors have explored this system.[35–37] There are several examples where this concept of reactive growth was used to produce monolithic ceramic bodies and high-density thin films with very modest temperature budgets.[38] For example, Akyıldız et al. demonstrated dense $BaTiO_3$ thin films produced from nanostructured Ti-metal precursor layers that were reacted hydrothermally with $Ba(OH)_2$ solutions.[39] Very recently Vakifahmetoglu et al. demonstrated the new process of Reactive Hydrothermal Liquid-Phase Densification (rHLPD) of bulk $BaTiO_3$.[40] In this process, TiO_2 precursor preforms are infiltrated with a $Ba(OH)_2$–$8H_2O$ solution and hydrothermally reacted over a range of temperatures and times. $BaTiO_3$ ceramics with 90% theoretical density could be produced using this method after ~70 h. For this method, it is important to have hydrothermal reactions with products of higher molar volume so as to fill initial pore space, absent transport processes that bring particle centers together.

There are similarities that link the CSP, HPP, and rHPLD. The most notable include a liquid phase that facilitates transport, and a series of dissolution and precipitation events between and among the original grains. There are however differences separating this family of

https://doi.org/10.1557/jmr.2017.262 Published online by Cambridge University Press

methods. For instance, CSP is a dynamic process (i.e., some of the liquid escapes as densification occurs) involving a single solid phase where transport is directed by gradients in pressure and concentration, while rHPLD is a reactive process where the initial solid and liquid phases react to create a new low-porosity polycrystalline product. In comparison, HPP, which was demonstrated first, is a more narrowly defined subset of CSP which requires uniaxial pressure, elevated temperature, hydrothermal conditions, and the initial powder is the source of mobile ions. By definition, CSP encompasses a broader set of densification pathways that involve nonaqueous liquids or vapors, liquid phase "cocktails" preloaded with mobile ionic species, and room-temperature pressure-less processes where high dissolution rates and intergranular capillary forces promote near-full density.

The ability to explore, identify, and understand the CSP landscape is now possible given the extensive literature base on sintering, hydrothermal synthesis, geology, and inorganic aqueous chemistry. To date, our experiments suggest a two-stage process whereby the particle compact first densifies by mechanical compaction, and subsequently densifies by a combination of homogeneous and heterogeneous precipitation events on existing and newly formed grains respectively. The participation of an intermediate glassy/gel-like grain boundary phase is likely present in some situations, particularly when crystallization is kinetically limited. The second stage follows saturation of the liquid phase with the constituent cations and anions, under constant pressure and temperature conditions—in this respect, there are many similarities to hydrothermal growth. While speculation remains regarding the microscopic driving force(s) for densification, current experiments suggest that a combination of curvature gradients, pressure gradients, and external strain contribute. It is important to note that the CSP is dynamic; small quantities of liquid can escape the die, finite liquid evaporates during high pressure, and the polycrystalline bodies or composites undergo densification. These dynamic aspects must be present and must be understood to regulate and optimize the process.

The mechanisms of cold sintering are in an early stage of understanding, the best practices for cold sintering are developing rapidly, and quantifiable links between chemical formulation and suitability for cold sintering are just emerging. Despite its relative youth as a ceramic process, cold sintering can produce a number of refractory ceramics with density values spanning ~85% to full theoretical density at temperatures below 300 °C. The maximum density values currently achieved depend upon the compatibility of the particular formulations with CSP and the maturity of individual process flows.

In the following three sections the authors present a summary of research activities that highlight: (i) the spectrum of materials that have been explored with initial comments regarding properties; (ii) a specific discussion of cold sintering mechanisms as they are understood today in the context for case studies for Li_2MoO_4 and ZnO; and (iii) a perspective on challenges, opportunities, and applications for cold sintered products.

III. THE SPECTRUM OF COLD SINTERED CERAMICS

Recently, a broad number of ceramic compositions that can undergo a CSP were reported.[12–28] In most cases, the process requires between 15 and 60 min under uniaxial pressures between 100 and 500 MPa. Over 50 inorganic compositions show evidence of CSP-enhanced densification, including binary, ternary, and quaternary compositions from oxide, bromide, chloride, fluoride, phosphate, and carbonate chemistries. For compositions that are most suited to CSP and for which methods are best developed, density values approach the theoretical limit. As with thermal sintering, some materials readily approach full density while others are more resistant to densification. Section IV discusses some of the composition relationships to cold sintering as we understand them today. Table I

TABLE I. Inorganic materials (with their space groups) sintered to date using the cold sintering process. A reproduction based on Ref. 12.

Binary compounds	Ternary compounds	Quaternary compounds	Quinary compounds
MoO_3 ($P2_1/c$)	Li_2CO_3 ($C2/c$)	$LiFePO_4$ ($Pnma$)	$LiAl_{0.5}Ge_{1.5}(PO_4)_3$
WO_3 ($P2_1/n$)	$CsSO_4$	$LiCoPO_4$ ($Pnma$)	$Li_{0.5x}Bi_{1-0.5x}Mo_xV_{1-x}O_4$
V_2O_3 ($R\bar{3}c$)	Li_2MoO_4 ($R\bar{3}$)	KH_2PO_4 ($Fdd2$)	...
V_2O_5 ($Pmmn$)	$Na_2Mo_2O_7$ ($Cmca$)	$Ca_5(PO_4)_3(OH)$ ($P6_3/m$)	...
ZnO ($P6_3mc$)	$K_2Mo_2O_7$ ($P\bar{1}$)	$(LiBi)_{0.5}MoO_4$	...
Bi_2O_3 ($P2_1/c$)	$ZnMoO_4$ ($P\bar{1}$)	...	...
CsBr ($Pm\bar{3}m$)	$Gd_2(MoO_4)_3$ ($Pba2$)	...	...
MgO ($Pm\bar{3}m$)	Li_2WO_4 ($R\bar{3}$)	...	...
PbTe ($Pm\bar{3}m$)	Na_2WO_4 ($Fd\bar{3}m$)	...	...
Bi_2Te_3 ($R\bar{3}m$)	$LiVO_3$ ($C2/c$)	...	...
NaCl ($Fm\bar{3}m$)	$BiVO_4$ ($C2/c$)	...	...
ZnTe ($F\bar{4}3m$)	$AgVO_3$ ($C2/c$)	...	...
AgI ($P6_3mc$)	Na_2ZrO_3 ($C2/c$)	...	...
CuCl ($F\bar{4}3m$)	$BaTiO_3$ ($P4mm$)	...	...
ZrF_4 ($C2/c$)	$NaNO_2$ ($Im2m$)	...	...
ZrO_2 ($P2_1/c$)	$Mg_2P_2O_7$ ($P2_1/c$)	...	...
...	$BaMoO_4$ ($I4_1/a$)	...	...
...	Cs_2WO_4 ($Pnma$)	...	...
...	$Na_xCo_2O_4$	...	...
...	$Ca_3Co_4O_9$ ($C2/m$)	...	...
...	KPO_3 ($Pa\bar{3}$)	...	...

https://doi.org/10.1557/jmr.2017.262 Published online by Cambridge University Press

provides a list of cold sintered compositions, specific aspects of preparation and properties are available in the references.

The interest in and utility of cold sintering is amplified by an expanded ability to integrate across conventional material classes, providing novel methods to assemble composites and join materials, opportunities for near-net shape fabrication, and new approaches to high density green bodies. While it is difficult to speculate on the number of formulations compatible with cold sintering, recent experiments reveal a growing population. Combining this list with the possibilities to expand integration suggests an exciting materials frontier to explore and exploit.

As an attempt to summarize and articulate this vision, Fig. 1 shows a diverse collection of CSP ceramics that have already been investigated in different sintered forms, including printed thick multilayer co-sintered structures, ceramic/polymer composites, and organic/inorganic composites. In addition to high densities, intriguing property responses are found in the materials fabricated by CSP. These observations have been demonstrated in a variety of functional materials that include ferroelectrics, ionic conductors, semiconductors, microwave dielectrics, thermoelectrics, structural ceramics, and Li-cathodes; in many cases it is possible to match the performance achieved with conventional high temperature sintering.[12–28] The organic/inorganic prototypes demonstrate new avenues to fabricate flexible electronics, as well as larger monolithic samples as shown in Fig. 1(g). The low temperatures which permit co-sintering of thermoplastics and ceramics also enable composite materials with low volume fractions of polymers that intercalate regions between well bonded ceramic grains.[19]

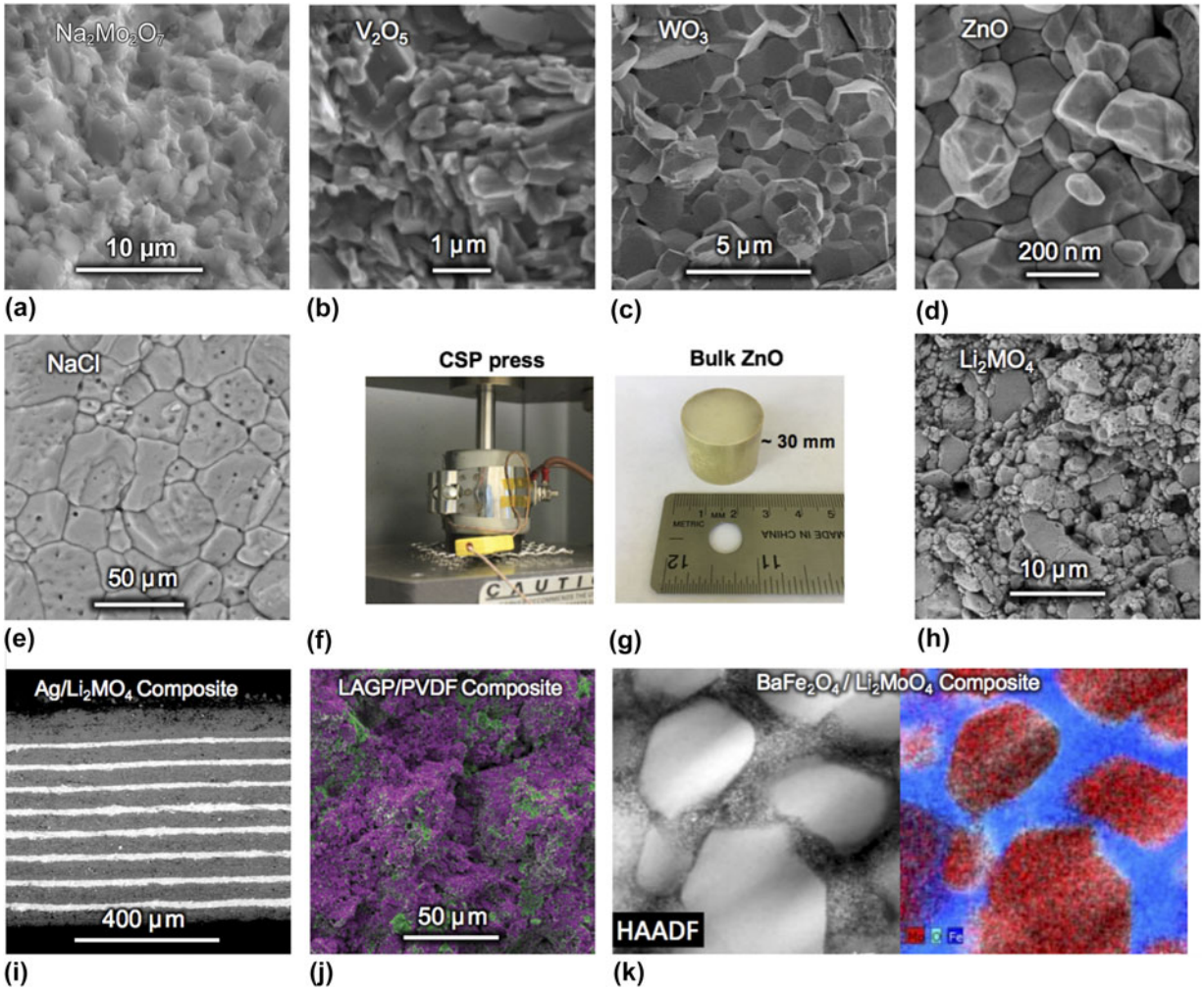


FIG. 1. (a–e), and (h) SEM fracture cross section images for cold sintered Na_2MoO_4, V_2O_5, WO_3, ZnO, NaCl, and Li_2MoO_4. In all cases, density values were above 94% theoretical; (f) photograph of cold sintering press with band heater on conventional pellet die; (g) image of large ZnO cylinder cold sintered to 97% theoretical density; (i) SEM cross section of cold sintered Ag/Li_2MoO_4 laminate; (j) SEM image with energy dispersive X-ray spectroscopy (EDS) false color showing the composite of LAGP and PVDF; and (k) TEM images of a cold sintered $BaFe_2O_4$/Li_2MoO_4 powder composite, high angle annular dark field and EDS contrast are shown.

https://doi.org/10.1557/jmr.2017.262 Published online by Cambridge University Press

IV. COLD SINTERING MECHANISMS AND CASE STUDIES

Based on the CSP experimental observations and analyses on multiple material systems to date, and the principles of classical ceramic sintering[1–3] and hydrothermal sintering theory,[11,41–43] we propose an initial model for cold sintering that comprises two stages: an initial stage, which is predominated by mechanical forces and particle rearrangement, and a second stage, which is predominated by pressure- and temperature-assisted dissolution and precipitation events that are driven by local and global gradients within the pellet die. We note that the division into two stages is a sensible convenience for discussing the phenomenon. In reality, several operative mechanisms appear to bridge the entire process. Figure 2 provides a schematic processing "timeline" for cold sintering. The intent of this figure is not to provide a specific set of events that occur in strict sequence, but to highlight the diverse number of compaction, consolidation, and densification mechanisms that may contribute to cold sintering.

In stage 1, densification is driven by uniaxial mechanical force, similar to conventional pressing, but there is assistance from the liquid phase associated with enhanced lubricity between particles. In stage 1, there is also the possibility for pressure driven solubility at the local scale where sharp particle facets come into contact; this facilitates interstitial space filling and greater surface area for particle sliding. Each of these factors can facilitate compaction as compared to the case of dry particles. In all situations, finite amounts of the initial liquid phase can escape the pellet die—the quantity depends on the specific material, the initial volume fraction, and the tolerance between die and punch—this is one of the several aspects that make cold sintering a dynamic process and is an important property to recognize, as noted by Yamazaki et al.[11]

Stage 2 is a proposed situation when elevated temperatures are applied under high constant pressure. Under these conditions, solubility is enhanced (as in the case of hydrothermal synthesis) and a supersaturated liquid is favorable to form. The supersaturation increases with time due to evaporation of the liquid phase from the pellet die which is not perfectly sealed. Unlike hydrothermal growth, however, an external uniaxial load is superimposed on the system providing the strain that promotes densification. The presence of this stress is critical, as it provides the driving force to bring particle centers together. The requirement is consistent with the argument of Riman's group that the hydrothermal transport in rHLPD has no driving force to bring particle centers together, rather, hydrothermal reactions fill intergranular space.[40] The uniaxial load also creates stress gradients at contacts between grains, thus an additional driving force for mass transport. As mentioned briefly in the introduction, generating a supersaturated liquid can occur by dissolution of the starting particles in an acidic or basic starting liquid, or by pre-loading the liquid phase with the cationic groups of interest. For example, ZnO can be cold sintered using an aqueous acetic acid solution or with a liquid comprised of dissolved zinc acetate.[26] This method can be particularly important for ternary compounds like $BaTiO_3$, where the cationic species have very different dissolution windows, or for oxides like Y_2O_3 which have very low solubility product constants.[44] For example, in the Y_2O_3 system, instead of adding an acidic liquid phase to pull Y^{3+} ions in solution, one can

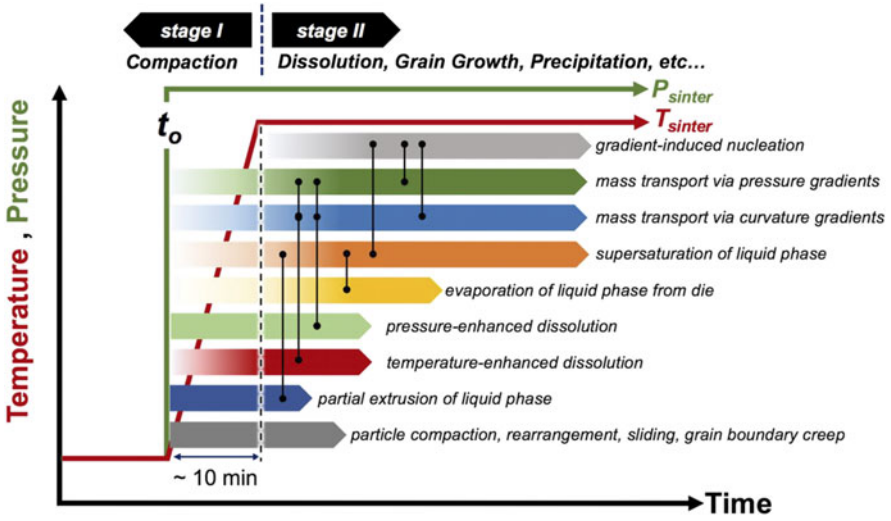


FIG. 2. Schematic illustration of the mechanisms that contribute to compaction, consolidation, densification, and crystallization during the cold sintering process. In this schematic temperature is increase after pressure application. Vertical black lines indicate processes/mechanisms that are coupled by a particularly strong interaction.

https://doi.org/10.1557/jmr.2017.262 Published online by Cambridge University Press

use a liquid phase of $Y(NO_3)_3$ dissolved in water. Note that while this will create a population of mobile species, it does not guarantee they will participate in mass transport. This engineered-solution approach to cold sintering has only been applied to a modest subset of compositions, but it may become an enabling route, particularly for low solubility compounds.

As evaporation and liquid extrusion progress, one expects increasing supersaturation in the remaining liquid phase. At this stage, the system is likely to respond in at least three possible routes. The first is heterogeneous nucleation, where dissolved species precipitate on surface sites with lower chemical potential. This process minimizes free energy by reducing surface area and ultimately by replacing solid–liquid interface with solid–solid grain boundary interfaces as the interparticle interstitial volumes are filled.[45]

The second route is homogeneous nucleation, where new crystals precipitate in the interstitial space between grains. Possibly, pressure gradients and or chemical gradients in this space and a very high degree of supersaturation promote this mechanism.[46] Fig. 3 shows an SEM image of cold sintered MnO where two distinct grain size populations are evident. The larger population with ~2 μm average diameter corresponds to the initial powder, while the much smaller population with <100 nm diameter, and are those which formed during cold sintering. This pellet was cold sintered at 250 °C under 300 MPa of pressure for 30 min. An acetic acid based liquid phase with a mass percentage of 5% (with respect to the powder) was used. The starting powder (Alpha Aesar 99% pure) was ball-milled for 24 h to achieve an average grain size of ~2 μm.

The third route involves a step-wise transition, whereby a metastable glass phase or intermediate compound is formed to bridge the initial solutes and final product. This process is well known in geochemistry of sedimentary rock formation and is often referred to as the Oswald Step Rule.[45] Evidence for this step-wise route is observed by Guo et al., in the $BaTiO_3$ system where an amorphous phase precipitates between the $BaTiO_3$ grains, as shown in Fig. 4. This phase can be converted subsequently with thermal energy into crystalline barium titanate.[13–15] EDS mapping in TEM reveals that the intergranular amorphous phase is carbon rich and contains both Ba and Ti cations. Proposed mechanisms for thermal conversion to $BaTiO_3$ are provided in the original manuscript, and are consistent with a dissolution-precipitation mechanism.[6]

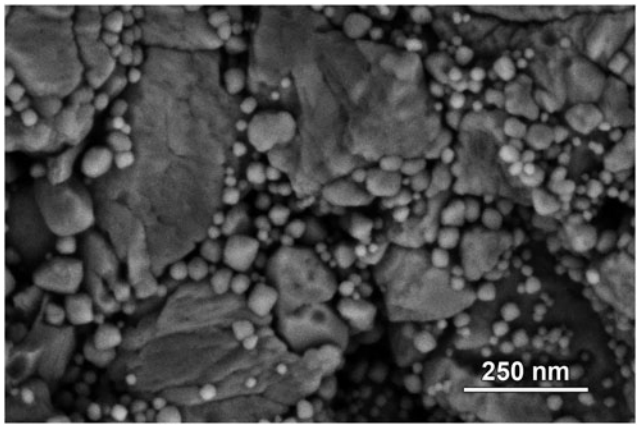


FIG. 3. SEM image of cold sintered MnO, densified at 250 °C and 530 MPa using an acetic acid-based liquid phase to a final density of 95% theoretical. The population of small grains were nucleated during CSP.

In some cases, particularly those with very high solubility in the liquid phase, an external pressure is not necessary for cold sintering. This has been observed for NaCl in which case capillary forces between particles likely provide the driving for densification.[12]

The discussion above is a proposal for the mechanisms that regulate cold sintering. It is important to note that these mechanisms are consistent with multiple data sets observed in numerous multiple compositions, but additional experiments are required to test the underlying hypotheses. At this stage, the primary intent is to articulate the potential spectrum of behaviors seen in a diverse collection of ceramic formulations.

In the following sub-sections we provide a more specific set of observations for cold sintered Li_2MoO_4 (LMO) and ZnO. We choose LMO and ZnO because they are particularly compatible with the CSP and enable unique opportunities to explore the roles of pressure, temperature liquid content, solvent, and time. While these trends will not apply to all cold sintered formulations, they provide a self-consistent set of process-property relationships.[12–28]

A. Case Study 1: LMO pressure and temperature effects

LMO was one of the initial materials for which cold sintering was observed, thus we chose it to demonstrate certain densification trends.[22–24] Data shown below was collected using commercial Li_2MoO_4 powders from Alfa-Aesar. Powders were ball milled for 24 h in methanol to achieve an average grain size of approximately 2 μm. The powders were dried post milling and stored at 100 °C to maintain the dehydrated state. The liquid vehicle for cold sintering in this case was pure water. The liquid phase was added by vapor infiltration, i.e., powders were exposed to water vapor by passing dry nitrogen through a room temperature bubbler filled with deionized water. Massing the powders before and after the bubbler treatment was used to quantify water content.

An initial experiment explored the importance of uniaxial pressure. Identical quantities of LMO powder

https://doi.org/10.1557/jmr.2017.262 Published online by Cambridge University Press

saturated with 3 mass% of water were loaded into a 1/2 inch steel die at room temperature and pressed in a hydraulic press between 180 and 700 MPa for a 30 min isoplethal dwell. The SEM images in Fig. 5(a) show the resulting fracture cross sections. In general, final densities increased with increasing pressure, however above 530 MPa residual cracking was observed. We thus identify pressures around 500 MPa as optimal for this particular powder. Dwell time at maximum pressure was also tested for the 530 MPa pressure and 3 mass% water content conditions. The results are shown in Fig. 5(b), where "wet density" is the density of the samples immediately after die extraction and "dried density" is the density of the samples after drying at 100 °C for 24 h. For sintering at room temperature, we find that most densification occurs within the first 10 min, then approaches completion in about 20 min.

As a second experiment, a set of powders was pressed at room temperature as a function of water content from nominal (i.e., no intentional water added) to 4.4 mass%. The results of this experiment are shown in Fig. 6. As seen from the nominal case, an already high density of 84% theoretical was achieved, and likely due to residual water not driven out by the 100 °C drying step. At 2 mass

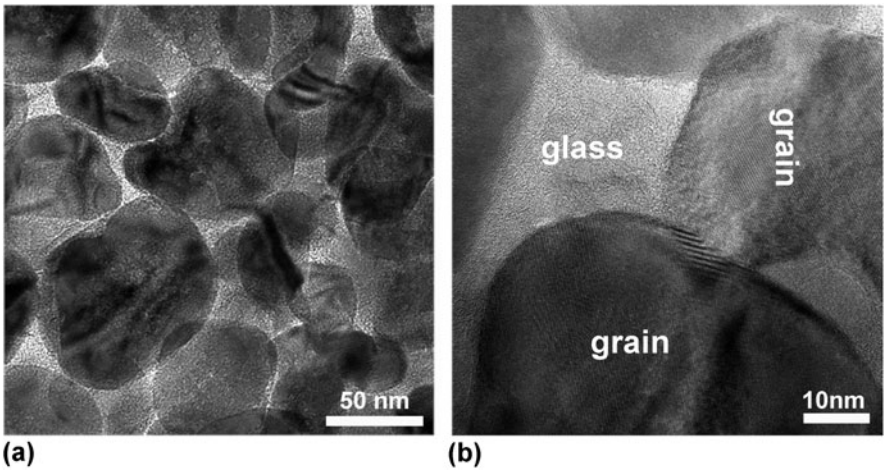


FIG. 4. (a–b) TEM micrographs of cold sintered $BaTiO_3$ (cold-sintered at 180 °C), where an intermediate amorphous phase occupies the interstitial space. This amorphous phase is carbonate rich, as determined by EDS chemical mapping. Reproduction from Ref. 15.

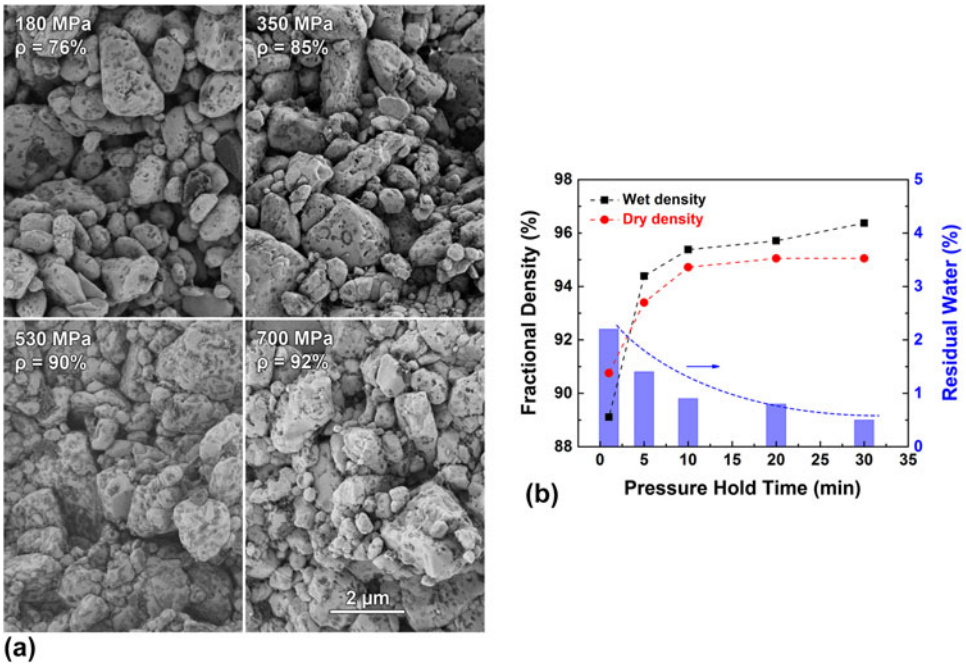


FIG. 5. (a) SEM images of LMO cross sections cold sintered at RT as a function of pressing pressure. All starting powders contained 3 mass% water. (b) Fractional density of LMO pellets pressed at 530 MPa with 3 mass% water as a function of dwell time at max pressure.

https://doi.org/10.1557/jmr.2017.262 Published online by Cambridge University Press

% water, density increases to 90%, with clear faceting seen in the fracture surface, suggesting precipitation/crystallization events. The density plateaus above 2 mass% water, but second phases appear in the fracture cross sections for these high water content powders. For LMO with high water content, diffraction data shows the presence of hydrated Lithia phases, suggesting that under these pressing conditions water is incorporated into ceramic as second phases which presumably become trapped. This series illustrates the dynamic aspect of cold sintering during which the liquid phase needs to be extruded.

Using the optimized pressure of 530 MPa, water content of 2 mass%, and dwell time of 30 min, a final sample set was prepared as a function of temperature. For this experiment, a resistive band heater was attached to the stainless steel die. Powders were loaded into the cold die, uniaxial pressure was applied, and the heater was turned on immediately and regulated to dwell at the desired final temperature. For temperatures in the range of 100 °C it took approximately 8 min for the temperature to stabilize. For this experiment three temperatures were evaluated: RT, 70, and 110 °C. The results are shown in Fig. 7. In general, higher temperatures promoted higher densities, and a 110 °C dwell produced a density of 99% theoretical, as measured using the Archimedes method.

From this brief case study, it is possible to appreciate the processing space available to cold sintering and the opportunities for process optimization given the combination of time, temperature, and solvent. While the

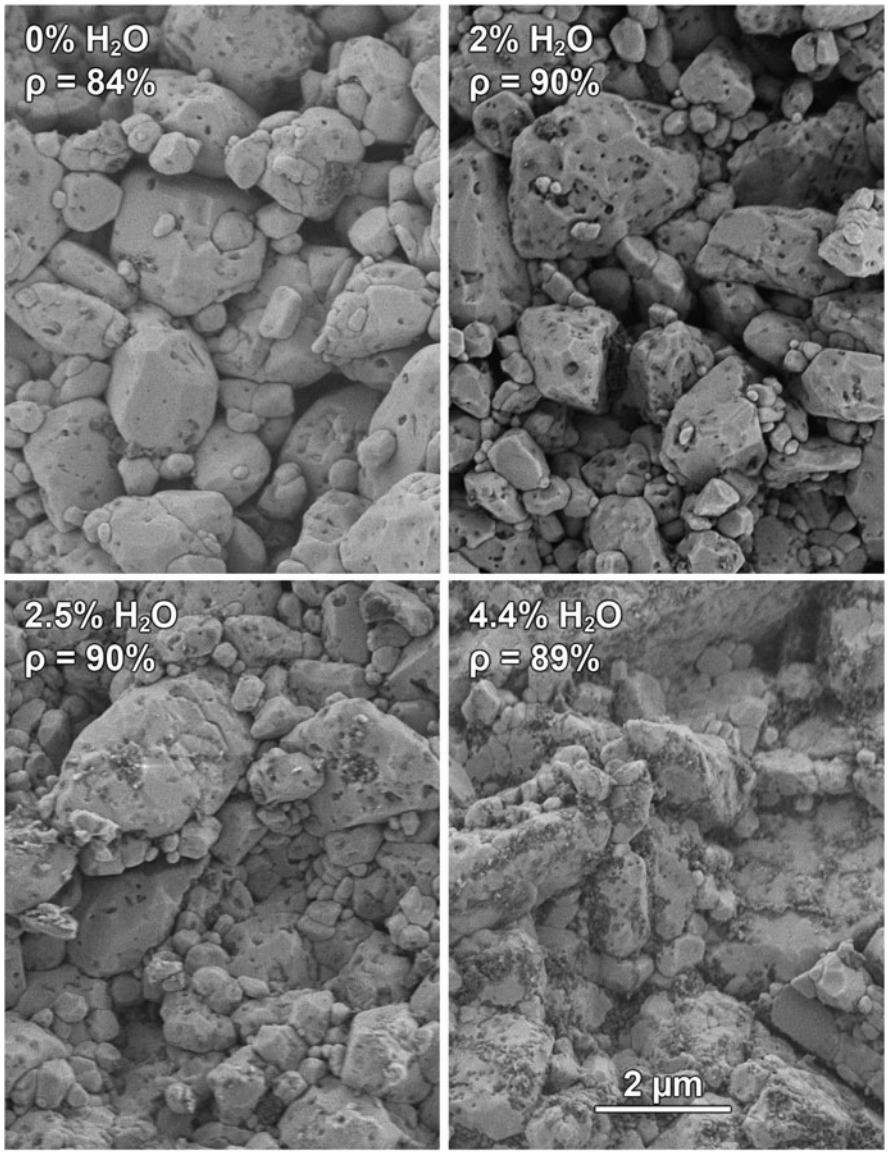


FIG. 6. SEM images of LMO cross sections cold sintered at RT as a function of water content. In each case a pressure of 530 MPa was used for densification.

https://doi.org/10.1557/jmr.2017.262 Published online by Cambridge University Press

combination of 530 MPa, 110 °C, and 2 mass% H_2O used above provides a route to near full density, it is likely that other combinations promote the same microstructural outcomes. This potential flexibility of process contributes to the excitement for CSP.

B. Case Study 2: ZnO grain growth

ZnO can be readily sintered by CSP by adding a 1 M acetic acid solution and/or dissolved zinc acetate as a transient liquid phase. High densities can be obtained for the ZnO system, in manners that are similar to the above strategies for Li_2MoO_4. Owing to its binary composition, the mobility of Zn^{2+} ions in solution, substantial solubility in many solvents, and a comparatively unstable hydroxide phase, ZnO is particularly well suited for cold sintering in aqueous systems and density values approaching 100% theoretical are possible with very uniform microstructures and clean grain boundaries.[26,27] Fig. 8 shows representative examples of ZnO cold sintered at 150 °C in the presence of a zinc acetate liquid phase under uniaxial pressure of 500 MPa.

The facility to cold sinter ZnO provides a unique opportunity to study the process within the classical understanding of conventional sintering and to compare the parameterization of factors used to understand the mechanisms. One particularly important comparison is grain growth.

Grain growth is an important process to monitor given its intimate link to densification—both are promoted by the desire to minimize surface area and curvature and there are existing relationships known for thermal sintering.[1–3] As such, monitoring grain growth can reveal distinct aspects of densification that enable one to distinguish between a consolidation process driven through creep or superplastic deformation (that could exist under high pressures and with nanoparticles), and a process driven by mass transport. To do so, a series of ZnO ceramics were prepared by CSP with a 10 wt% addition of 1 M acetic acid aqueous

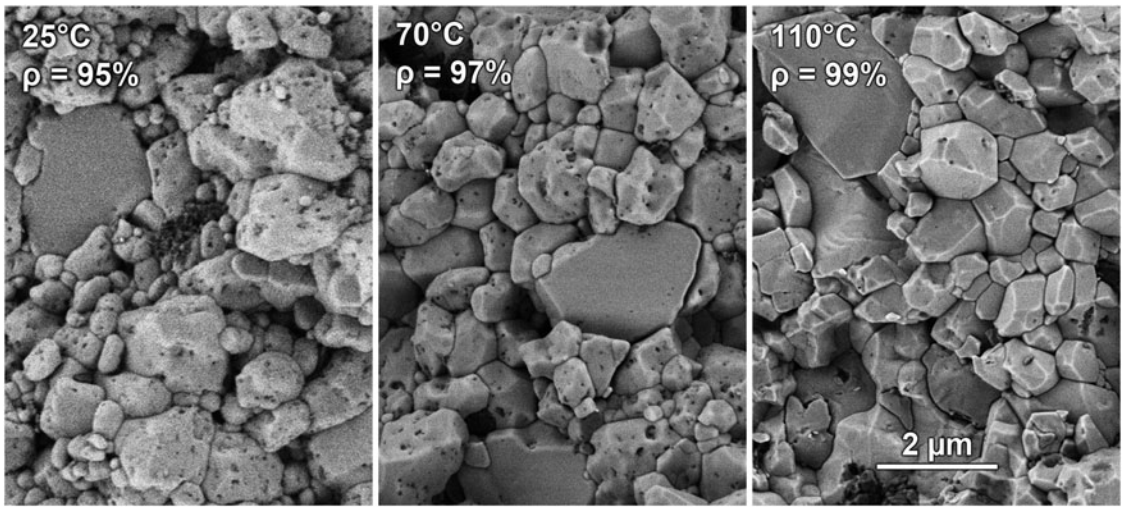


FIG. 7. SEM images of LMO ceramics cold sintered with increasing temperature, at 530 MPa and 2 mass% H_2O, and a progression of density values that approaches the theoretical limit.

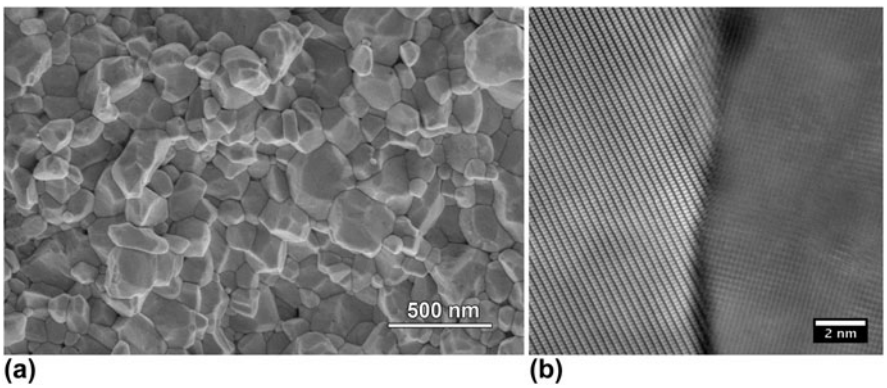


FIG. 8. (a) SEM and (b) STEM images of ZnO cold sintered with Zn-acetate solution to near theoretical density. Note the clean and highly crystalline structure in the vicinity of grain boundaries.

https://doi.org/10.1557/jmr.2017.262 Published online by Cambridge University Press

solution pressed over a temperature range spanning 120–300 °C. All samples were pressed at a constant pressure of 350 MPa, with times ranging from 30 min to 5 h. The average starting ZnO particle size was 200 nm. A series of SEM images from ZnO fracture cross sections was used to determine average grain diameter.

For conventional heat treatments, we understand the coarsening process to follow the relationship in Eq. (1):

$$G^N - G_0^N = tK_0 \exp(Q/RT) \quad , \qquad (1)$$

where G_0 is initial grain size, t is the sintering time, and N is the kinetic grain growth exponent, K_0 is a constant, Q is the apparent activation energy for grain growth, R is the gas constant, and T is the absolute temperature. It is important to note that samples cold sintered for 30 min exhibited density values above 98%.[26] As such, mass transport occurring over longer durations was associated primarily with grain growth and the assumptions associated with the relationship above, i.e., coarsening independent of densification apply. Equation (1), can be rearranged as Eq. (2);

$$\log G = (1/N)\log t + (1/N)[\log K_0 - 0.434(Q/RT)] \quad , \qquad (2)$$

which provides a linear relationship between average grain size and time for constant-temperature conditions. When applied to our data set, this expression enables one to calculate the kinetic grain growth exponent N, as shown in Fig. 9(a) from which a value of 3 is found. We note that a grain growth exponent of 3 is characteristic of systems that coarsen via a liquid phase.[1–3] Eq. (3) is derived by substituting $N = 3$ and the starting grain size into Eq. (1),

$$\log\left(G^3/t\right) = \log K_0 - 0.434(Q/RT) \quad . \qquad (3)$$

From Eq. (3) and the temperature dependent data set, one can calculate the activation energy Q as shown in Fig. 9(b).

The important outcome of this treatment is that under these CSP conditions the final stage of sintering has grain growth kinetics that follow classical behavior, i.e., an exponent $N \sim 3$, but with an activation energy that is substantially smaller than previously reported for conventional sintering.

Provided a consistent sintering mechanism over the temperature window between 120 and 300 °C, the grain growth activation energy, as calculated from the slope of Fig. 3(b), is 43 kJ/mol. In comparison, Senda and Bradt, report an activation energy for conventionally sintered pure ZnO of 200 kJ/mol, nearly five times larger than required for CSP.[47] This comparison suggests that ZnO cold sinters by a mechanism analogous to liquid phase sintering, whereby the second phase provides a transport pathway with a reduced activation energy, Q, which enhances grain boundary mobility.

As research on cold sintering expands, it will be important to extend these investigations to many other systems as a function of liquid phase composition, solute concentration, and temperature. While this classical treatment of grain growth kinetics fits the ZnO dataset well, it is possible that other systems behave differently. Exploring these trends will provide critical insights that improve understanding and predictive power.

V. COLD SINTERING PERSPECTIVES, CHALLENGES AND OPPORTUNITIES

A. Perspectives

Ceramics have been manufactured via thermal sintering by humans since the upper Paleolithic era.[48] Since

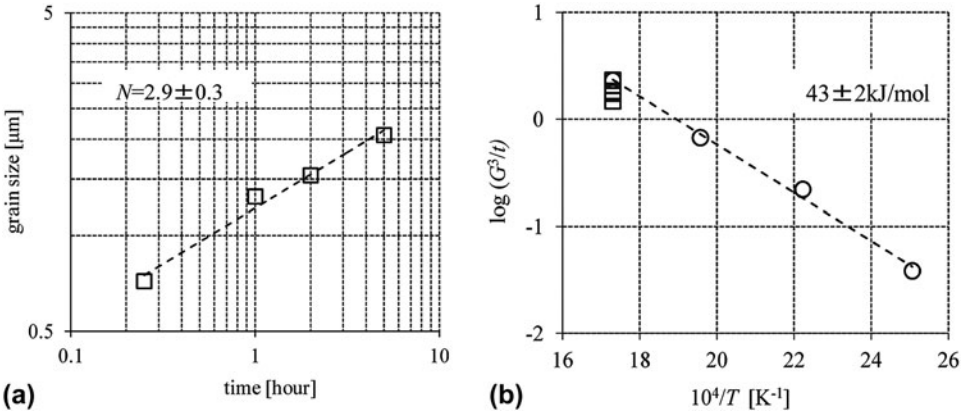


FIG. 9. (a) Plot of the isothermal log–log grain growth showing the power exponent of $N \sim 3$, and (b) Arrhenius plot of the grain growth process with an activation energy of 43 kJ/mol, much lower than the reported conventional energies of 200 kJ/mol for ZnO.[26]

https://doi.org/10.1557/jmr.2017.262 Published online by Cambridge University Press

then, sintering has relied most commonly on the application of high temperature to promote mass transport and create a dense and robust body. This high temperature requirement established a framework for implementation, formation, and integration of ceramics that persisted for nearly 30,000 years. High temperature processing routes, often in oxidizing environments, create challenges for achieving arbitrarily small grain sizes, for maintaining high purity, and for integrating ceramics, metals, and polymers. As the Materials Research community embraces an increasingly interdisciplinary approach, there are needs for synthesis tools that facilitate new levels of material integration. Cold sintering is a potential enabler for this 21st century vision of advanced materials. If the research community demonstrates cold sintering across a broad family of compositions with properties comparable to conventional parts, the following broad impacts are conceivable:

(i) Reduced energy consumption by a dramatically lower thermal budget.
(ii) Integration between diverse inorganic materials: Compositions that typically exhibit exclusive densification process windows (i.e., oxides and nitrides) can be co-prepared in a single monolith.
(iii) Integration between diverse grain sizes/structures: Microstructures that feature macro-, micro-, and nano-size grains can be prepared in one step.
(iv) Organic/inorganic composites in a one-step process: the extreme low temperatures are compatible with many polymers.
(v) Near-net shape fabrication: dense polycrystalline parts take precisely the same shape as their parent dies—"stamping" textures and patterns is possible.
(vi) New scientific learning and new engineering principles that will help to shape a new synthesis/manufacturing infrastructure.

It is clear that this process is in the early stages of development and substantial learning is needed at many levels to appreciate these impacts. This will likely require that researchers and educators embrace diverse subfields including, geochemistry, colloidal science, crystal growth, polymer science, ceramic science, and nonequilibrium thermodynamics. The complexity of the process will probably require contributions from materials modeling and simulation efforts.

B. Challenges

Challenges for cold sintering technology exist scientifically and industrially. The most pressing scientific challenges are associated with our beginner's knowledge of densification in the presence of pressure, temperature, and ions in solution, and our appreciation for the dynamic nature of this process. The importance of many factors need to be addressed: examples of which we are aware include grain size, grain morphology, particle size distribution, die sealing, rate of pressure application, and liquid phase viscosity. For select materials we understand several of these factors, but a generalized framework that can be applied to many compositions needs developing. While there are many formulations amenable to cold sintering, there is an equal number that challenge the process. In particular, extremely low solubility binary oxides like Ta_2O_5, ternary compounds with very disparate cation solubilities like $LaNbO_3$, and compounds with very stable hydroxides or carbonates like MgO and CaO respectively, provide significant processing challenges. These challenges, however, are not fundamental, rather they are limitations presented by incomplete understanding and unexplored processing space. For example, hydroxide and carbonate phases can be mediated by an alternative liquid phase. We have only scratched the surface of cold sintering experimental space and anticipate rapid advances as additional researchers engage the opportunity.

Cold sintering involves a substantial departure from convention, and as such it will take some time to gain acceptance in the materials preparation community. Materials scientists recognize high temperature as one of the most influential and important processing parameters. It provides the energy to overcome activation barriers for transport, chemical reactions, and defect formation, and is the multiplier for all entropic contributions. Consequently, it is necessary to rigorously validate materials and their properties when they are made without it. To meet this challenge, it will be necessary to duplicate synthesis and property measurements in independent laboratories to generate confidence.

From an industrial perspective, cold sintering requires a substantially different infrastructure compared to conventional methods. From initial experiments it is clear that investments are also needed to advance for cold sintering instrumentation, particularly to develop methods that can be scaled. Additionally, the community will need statistically relevant property/performance validation on the industrial side. In this context, it is interesting to consider introducing other energetic perturbations to facilitate CSP: applying electric fields or acoustic energy are enticing future options.

The ability to fabricate ceramic/polymer composites is a particularly appealing feature of CSP. If these laboratory methods can be scaled for compatibility with the plastics industry tremendous impact is expected. Lower uniaxial pressures, and injection molding strategies would offer additional appeal.

C. Opportunities

Cold sintering creates opportunities to combine materials that previously would chemically react, decompose, or volatilize in a dense and robust form factor.

https://doi.org/10.1557/jmr.2017.262 Published online by Cambridge University Press

Consequently, there are excellent possibilities to develop unique bulk materials, multilayers, and thick films. The constituent materials can encompass inorganics, nanomaterials, biomaterials, polymers, quantum dots, 2-D materials, liquid crystals, phosphors, Metal-Organic-Frameworks (MOFs), etc., and create new multifunctionality within new composite and device designs. We recognize that much additional work is needed to realize this materials-agnostic vision for integration, but even at this early stage it is conceivable that such capabilities would impact numerous technology areas, some of these opportunities are listed in Table II.

As an initial example, Guo et al. showed that ceramic and polymer material technologies can unite using CSP. Particularly to design composites with 1–30 vol% of polymers in a dense ceramic matrix.[19] There are a wide range of thermoplastic powders that can be mixed and dispersed with the ceramic particles. CSP experiments demonstrate that such composites are attractive as dielectrics for electronic packaging, electrolytes, and electrodes for electrochemical systems, and semiconductor composites. Ultimately, an expanded ability to integrate dissimilar materials with a broader property spectrum leads to performance characteristics that address expanded technology needs. We believe cold sintering will be an important approach to achieve this goal.

TABLE II. Potential applications for CSP. An adaptation from Ref. 19.

Electroceramics	Mechanical	Refractories
Chemical sensors	Abrasives	Architectural ceramics
Electrocalorics	Bearings	Glass
Electrochemical cells	Catalyst supports	Crucibles
Electronic packaging	Ceramic-metal seals	Refractory bricks
Flexible electronics	Coatings	Whitewares
Magnetic inductors and transformers	Cutting tools	...
Multilayer passive components	Filters	...
Piezoelectrics	Milling media	...
Pyroelectrics	Packaging	...
Resistors and resistive heaters	Proppants	...
Solar cells	Valves	...
Superconductors	...	...
Thermistors and varistors	...	...
Thermoelectrics	...	...

Cold sintering may provide new approaches to design grain boundary structure. Applications of interest include barrier layer capacitors with colossal permittivities, and varistor materials for circuit protection. These types of electroceramics exhibit strong contrast in conductivity between the grain interiors and grain surfaces/boundaries, and often benefit from a nanoscaled microstructure. The low thermal budget of cold sintering can facilitate a microstructure that favors small sizes, minimizes chemical interactions, and preserves the properties of the initial powders. We can also prepare composites with co-tuned dielectric and magnetic properties. Figure 10 shows two examples where cold sintering combines dissimilar materials with vastly different grain sizes; nanoferrite $BaFe_{12}O_{19}$ and nanoferroelectric $BaTiO_3$ dispersed among micron-sized grains of Li_2MoO_4. Such composite designs enable tunable permittivity and permeability, which are important parameters for impedance matching in high frequency antennae.

Ideally, with cold sintering, materials can be selected based on the desired properties, unencumbered by considerations of compatible process windows. This may open the design space to regions previously inaccessible.

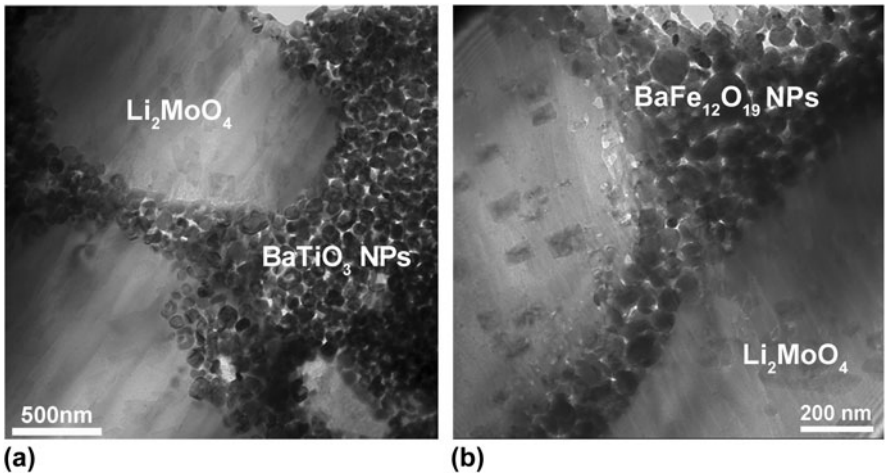


FIG. 10. TEM images demonstrating how cold sintering can be used to develop a unique composite microstructure in two-phase mixtures; (a) a $Li_2MoO_4/BaFe_{12}O_{19}$ nanocomposite; and (b) a $Li_2MoO_4/BaTiO_3$ nanocomposite.

https://doi.org/10.1557/jmr.2017.262 Published online by Cambridge University Press

VI. CONCLUSIONS

Dense refractory ceramics can be prepared at temperatures below 300 °C when assisted by uniaxial pressure and an engineered liquid phase. While not completely understood, the mass transport mechanisms that promote densification combine aspects of liquid phase sintering, hot pressing, and hydrothermal dissolution/precipitation. This process, now referred to as cold sintering, has been demonstrated in over 50 compositions. Just as in thermal sintering there is a spectrum of material compatibility. In some compositions, like ZnO, density values can be easily driven to near theoretical limits due to substantial solubility and fast kinetics. In other systems, like $BaTiO_3$, differential dissolution of constituent cations and the potential for reactions with aqueous solutions demand more sophisticated approaches. While much remains to be learned regarding the mechanisms of CSP and the properties of materials prepared in this manner, it is clear that creating dense ceramic bodies at near room temperature offers transformational opportunities for material integration, reduced energy consumption, near net-shape formation, composite design, and property engineering. The capabilities observed for CSP give cause to reconsider the historical perspectives on ceramic processing and to imagine new methods to manufacture ceramics with enhanced technological value and impact.

ACKNOWLEDGMENTS

The authors acknowledge support from The Center for Dielectrics and Piezoelectrics, a national research center and consortium under the auspices of the Industry/University Cooperative Research Centers program at the National Science Foundation under Grant Nos. IIP-1361571 and 1361503. The authors thank Professor James LeBeau and Matt Cabral for TEM imaging of cold sintered ceramics. This work was performed in part at the Analytical Instrumentation Facility (AIF) at North Carolina State University, which is supported by the State of North Carolina and the National Science Foundation (award number ECCS-1542015). The AIF is a member of the North Carolina Research Triangle Nanotechnology Network (RTNN), a site in the National Nanotechnology Coordinated Infrastructure (NNCI). We also thank the visiting scientist support from Murata Electronics, and also the Materials Characterization Laboratory, at the Materials Research Institute at PSU. This material is based upon work supported by the National Science Foundation Graduate Research Fellowship Program under Grant No. DGE-1252376. Any opinions, findings, and conclusions or recommendations expressed in this material are those of the author(s) and do not necessarily reflect the views of the National Science Foundation.

REFERENCES

1. M.N. Rahaman: *Sintering of Ceramics* (CRC Press, Baca Raton, 2008).
2. R.M. German: *Sintering Theory and Practice* (Wiley, New York City, 1996).
3. S-J.L. Kang: *Sintering: Densification, Grain Growth, and Microstructure* (Butterworth-Heinemann, Oxford, 2005).
4. M. Cologna, B. Rashkova, and R. Raj: Flash sintering of nanograin zirconia in <5 s at 850 °C. *J. Am. Ceram. Soc.* **93**(11), 3556 (2010).
5. Z. Shen, Z. Zhao, H. Peng, and M. Nygren: Formation of tough interlocking microstructures in silicon nitride ceramics by dynamic ripening. *Nature* **417**, 266 (2002).
6. R. Chaim, A. Shlayer, and C. Estournes: Densification of nanocrystalline Y_2O_3 ceramic powder by spark plasma sintering. *J. Eur. Ceram. Soc.* **29**(1), 91 (2009).
7. Z. Valdez-Nava, S. Guillemet-Fritsch, C. Tenailleau, T. Lebey, B. Durand, and J.Y. Chane-Ching: Colossal dielectric permittivity of $BaTiO_3$-based nanocrystalline ceramics sintered by spark plasma sintering. *J. Electroceram.* **22**(1–3), 238 (2009).
8. C. Elissalde, M. Maglione, and C. Estournes: Tailoring dielectric properties of multilayer composites using spark plasma sintering. *J. Am. Ceram. Soc.* **90**(3), 973 (2007).
9. N. Shomrat, S. Baltianski, C.A. Randall, and Y. Tsur: Flash sintering of potassium-niobate. *J. Eur. Ceram. Soc.* **35**(7), 2209 (2015).
10. Z. Zhao, V. Buscaglia, P. Bowen, and M. Nygren: Spark plasma sintering of nano-crystalline ceramics. *Key Eng. Mater.* **264–268**, 2297 (2004).
11. N. Yamasaki, K. Yanagisawa, M. Nishioka, and S. Kanahara: A hydrothermal hot-pressing method: Apparatus and application. *J. Mater. Sci. Lett.* **5**, 355 (1986).
12. J. Guo, H. Guo, A.L. Baker, M.T. Lanagan, E.R. Kupp, G.L. Messing, and C.A. Randall: Cold sintering: A paradigm shift for processing and integration of ceramics. *Angew. Chem., Int. Ed.* **55**(38), 11457 (2016).
13. H. Guo, A. Baker, J. Guo, C.A. Randall, and D. Johnson: Cold sintering process: A novel technique for low-temperature ceramic processing of ferroelectrics. *J. Am. Ceram. Soc.* **99**(11), 3489 (2016).
14. H. Guo, A. Baker, J. Guo, and C.A. Randall: Protocol for ultralow-temperature ceramic sintering: An integration of nanotechnology and the cold sintering process. *ACS Nano* **10**(11), 10606 (2016).
15. H. Guo, J. Guo, A. Baker, and C.A. Randall: Hydrothermal-assisted cold sintering process: A new guidance for low-temperature ceramic sintering. *ACS Appl. Mater. Interfaces* **8** (32), 20909 (2016).
16. A. Baker, H. Guo, J. Guo, and C. Randall: Utilizing the cold sintering process for flexible-printable electroceramic device fabrication. *J. Am. Ceram. Soc.* **99**(10), 3202 (2016).
17. J. Guo, A.L. Baker, H. Guo, M. Lanagan, and C.A. Randall: Cold sintering process: A new era for ceramic packaging and microwave device development. *J. Am. Ceram. Soc.* **7**, 1 (2016).
18. J. Guo, H. Guo, D.S.B. Heidary, S. Funahashi, and C.A. Randall: Semiconducting properties of cold sintered V_2O_5 ceramics and Co-sintered V_2O_5-PEDOT: PSS composites. *J. Eur. Ceram. Soc.* **37**(4), 1529 (2016).
19. J. Guo, S.S. Berbano, H. Guo, A.L. Baker, M.T. Lanagan, and C.A. Randall: Cold sintering process of composites: Bridging the processing temperature gap of ceramic and polymer materials. *Adv. Funct. Mater.* **26**(39), 7115 (2016).
20. H. Guo, J. Guo, A. Baker, and C.A. Randall: Cold sintering process for ZrO_2-based ceramics: Significantly enhanced densification evolution in yttria-doped ZrO_2. *J. Am. Ceram. Soc.* **100**(2), 491 (2016).

https://doi.org/10.1557/jmr.2017.262 Published online by Cambridge University Press

21. H. Guo, T.J.M. Bayer, J. Guo, A. Baker, and C.A. Randall: Cold sintering process for 8 mol% Y_2O_3-stabilized ZrO_2 ceramics. *J. Eur. Ceram. Soc.* **37**(5), 2303 (2017).
22. H. Kähäri, M. Teirikangas, J. Juuti, and H. Jantunen: Dielectric properties of lithium molybdate ceramic fabricated at room temperature. *J. Am. Ceram. Soc.* **97**(11), 3378 (2014).
23. H. Kähäri, M. Teirikangas, J. Juuti, and H. Jantunen: Improvements and modifications to room-temperature fabrication method for dielectric Li_2MoO_4 ceramics. *J. Am. Ceram. Soc.* **98**(3), 687 (2015).
24. H. Kähäri, M. Teirikangas, J. Juuti, and H. Jantunen: Room-temperature fabrication of microwave dielectric Li_2MoO_4–TiO_2 composite ceramics. *Ceram. Int.* **42**(9), 11442 (2016).
25. C.A. Randall, J. Guo, H. Guo, A. Baker, and M.T. Lanagan (The Penn State Research Foundation, assignee): Cold Sintering Ceramics and Composites. U.S. Provisional Patent Service Number **62/234** (2015).
26. S. Funahashi, J. Guo, H. Guo, K. Wang, A.L. Baker, K. Shiratsuyu, and C.A. Randall: Demonstration of the cold sintering process study for the densification and grain growth of ZnO ceramics. *J. Am. Ceram. Soc.* **100**(2), 546 (2017).
27. S.S. Berbano, J. Guo, H. Guo, M.T. Lanagan, and C.A. Randall: Cold sintering process of $Li_{1.5}Al_{0.5}Ge_{1.5}(PO_4)_3$ solid electrolyte. *J. Am. Ceram. Soc.*, **100**(5), 2123 (2017).
28. I.J. Induja and M.T. Sebastian: Microwave dielectric properties of mineral sillimanite obtained by conventional and cold sintering process. *J. Eur. Ceram. Soc.* **37**(5), 2143 (2017).
29. P. De Silva, L. Bucea, V. Sirivivatnanon, and D.R. Moorehead: Carbonate binders by "cold sintering" of calcium carbonate. *J. Mater. Sci.* **42**(16), 6792 (2007).
30. N. Yamasaki, W. Tang, and J. Ke: Low-temperature sintering of calcium carbonate by a hydrothermal hot-pressing technique. *J. Mater. Sci. Lett.* **11**(13), 934 (1992).
31. K. Yanagisawa, K. Ioku, and N. Yamasaki: Formation of anatase porous ceramics by hydrothermal hot-pressing of amorphous titania spheres. *J. Am. Ceram. Soc.* **80**(5), 1303 (1997).
32. K. Yanagisawa, K. Ioku, and N. Yamasaki: Pore size control of porous silica ceramics by hydrothermal hot-pressing. *J. Ceram. Soc. Jpn.* **102**(1190), 966 (1994).
33. Y. Xie, S. Yin, H. Yamane, T. Hashimoto, and T. Sato: Low temperature sintering and color of a new compound $Sn_{1.24}Ti_{1.94}O_{3.66}(OH)_{1.50}F_{1.42}$. *Solid State Sci.* **11**(9), 1703 (2009).
34. F. Bouville and A.R. Studart: Geologically-inspired strong bulk ceramics made with water at room temperature. *Nat. Commun.* **8**, 14655 (2017).
35. I.J. Clark, T. Takeuchi, N. Ohtori, and D.C. Sinclair: Hydrothermal synthesis and characterisation of perovskite. *J. Mater. Chem.* **9**(1), 83 (1999).
36. M.Z.C. Hu, V. Kurian, E.A. Payzant, C.J. Rawn, and R.D. Hunt: Wet-chemical synthesis of monodispersed barium titanate particles—Hydrothermal conversion of TiO_2 microspheres to nanocrystalline $BaTiO_3$. *Powder Technol.* **110**(1–2), 2 (2000).
37. P.K. Dutta, R. Asiaie, S.A. Akbar, and W. Zhu: Hydrothermal synthesis and dielectric properties of tetragonal $BaTiO_3$. *Chem. Mater.* **6**(9), 1542 (1994).
38. M. Yoshimura, S-E. Yoo, M. Hayashi, and N. Ishizawa: Preparation of $BaTiO_3$ thin film by hydrothermal electrochemical method. *Jpn. J. Appl. Phys.* **28**(11), 2007 (1989).
39. H. Akyıldız, M. Casper, S. Aygün, P. Lam, and J. Maria: Hydrothermal $BaTiO_3$ thin films from nanostructure Ti templates. *J. Mater. Res.* **26**(4), 592 (2011).
40. C. Vakifahmetoglu, J.F. Anger, V. Atakan, S. Quinn, S. Gupta, Q. Li, L. Tang, and R.E. Riman: Reactive hydrothermal liquid-phase densification (rHLPD) of ceramics—A study of the $BaTiO_3$[TiO_2] composite system. *J. Am. Ceram. Soc.* **99**, 3893 (2016).
41. S-I. Hirano and S. Somiya: Hydrothermal reaction sintering of pure Cr_2O_3. *J. Am. Ceram. Soc.* **59**(11–12), 534 (1976).
42. K. Anagisawa, M. Sasaki, M. Nishioka, K. Ioku, and N. Yamasaki: Preparation of sintered compacts of anatase by hydrothermal hot-pressing. *J. Mater. Sci. Lett.* **13**, 765 (1994).
43. B. Dargatz, J. Gonzalez-Julian, M. Bram, P. Jakes, A. Besmehn, L. Schade, R. Röder, C. Ronning, and O. Guillon: FAST/SPS sintering of nanocrystalline zinc oxide-part I: Enhanced densification and formation of hydrogen-related defects in presence of adsorbed water. *J. Eur. Ceram. Soc.* **36**(5), 1207 (2016).
44. W.M. Haynes: *CRC Handbook of Chemistry and Physics*, 97th ed. (CRC Press, Boca Raton, 2016).
45. R.A. Van Santen: The Ostwald step rule. *J. Phys. Chem.* **88**(6), 5768 (1984).
46. D. Velegol, A. Garg, R. Guha, A. Kar, and M. Kumar: Origins of concentration gradients for diffusiophoresis. *Soft Matter* **12**(21), 4686 (2016).
47. T. Senda and R.C. Bradt. Grain growth in sintered ZnO and ZnO–Bi_2O_3 ceramics. *J. Am. Ceram. Soc.* **1**, 106 (1990).
48. P.B. Vandiver, O. Soffer, B. Klima, J. Svoboda, P.B. Vandiver, O. Soffer, B. Klima, and J. Svoboda: The origins of ceramic technology at dolni věstonice, czechoslovakia. *Science* **246**(4933), 1002 (2017).

https://doi.org/10.1557/jmr.2017.262 Published online by Cambridge University Press